

Enhanced field emission from CuO nanowire arrays by *in situ* laser irradiation

Cite as: J. Appl. Phys. **102**, 114302 (2007); <https://doi.org/10.1063/1.2818096>

Submitted: 14 September 2007 . Accepted: 04 October 2007 . Published Online: 04 December 2007

Y. W. Zhu, C. H. Sow, and J. T. L. Thong



View Online



Export Citation

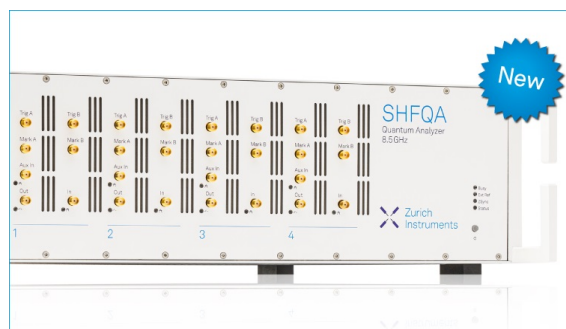
ARTICLES YOU MAY BE INTERESTED IN

[On the growth and electrical characterization of CuO nanowires by thermal oxidation](#)
Journal of Applied Physics **106**, 034303 (2009); <https://doi.org/10.1063/1.3187833>

[Study of field emission, electrical transport, and their correlation of individual single CuO nanowires](#)

Journal of Applied Physics **109**, 023710 (2011); <https://doi.org/10.1063/1.3536478>

[Excellent field emission properties of vertically oriented CuO nanowire films](#)
AIP Advances **8**, 045109 (2018); <https://doi.org/10.1063/1.5022320>



Your Qubits. Measured.

Meet the next generation of quantum analyzers

- Readout for up to 64 qubits
- Operation at up to 8.5 GHz, mixer-calibration-free
- Signal optimization with minimal latency

Find out more



Enhanced field emission from CuO nanowire arrays by *in situ* laser irradiation

Y. W. Zhu and C. H. Sow^{a)}

Department of Physics, National University of Singapore, Singapore 117542, Singapore and National University of Singapore Nanoscience & Nanotechnology Initiative, Singapore 117542, Singapore

J. T. L. Thong

Department of Electrical and Computer Engineering, National University of Singapore, Singapore 117576, Singapore and National University of Singapore Nanoscience & Nanotechnology Initiative, Singapore 117576, Singapore

(Received 14 September 2007; accepted 4 October 2007; published online 4 December 2007)

Laser irradiation was found to effectively enhance the field emission current of CuO nanowire arrays. The effects of laser intensity, wavelength, emission current, and working vacuum on the enhancement have been investigated in detail. The observed laser induced enhancement in field emission current is attributed to the interplay of two factors, namely, laser induced electron transition to excited states and surface oxygen desorption. Among these factors, the contribution from extra excited electrons, which increases the number of electrons in conduction band of CuO for subsequent tunneling, is dominant. A physical process of the laser induced enhancement is discussed. This work helps to elucidate the mechanisms of electron field emission from narrow band gap nanowires and will be useful for designing future vacuum nanodevices, such as photodetectors or switches, based on field emission of nanowires. © 2007 American Institute of Physics.

[DOI: [10.1063/1.2818096](https://doi.org/10.1063/1.2818096)]

I. INTRODUCTION

In the past few years, a wide range of nanowires has been studied as novel electron emitters due to their high aspect ratios, controllable electronic property, and chemical stability under harsh environments.¹ Among the nanowire field emitters, copper oxide (CuO) nanowires have attracted much interest due to their low turn-on field, high current density, and uniform emission images.^{2,3} Furthermore, CuO nanowires can be synthesized on a large scale by simply annealing Cu in ambience,^{4,5} providing opportunities to investigate the various effects on the field emission such as plasma etching^{6,7} and focused laser patterning.⁸ In addition, *p*-type CuO has a direct and narrow band gap (1.2–1.7 eV),^{9–12} making it very sensitive to thermal activation¹³ or light irradiation.¹⁴ Such a property could be exploited to fabricate useful devices such as CuO field emission based thermal or optical sensor and switch.

On the other hand, the interaction between laser and field emission has been an interesting topic for years. There are a few ways to approach this study. For example, after laser irradiation or treatments, carbon nanotubes¹⁵ and polymer film¹⁶ exhibit improved field emission performance, which is attributed to the modified morphology or tip structure, and cleaned surface. Another effect of laser is from the nondestructive *in situ* irradiation during field emission, which is known as photofield emission.¹⁷ Photofield emission combines the element of field emission and photoemission due to the irradiation with photon energy larger than the effective

work function of emitters,¹⁸ or results from the resonance between irradiation photons and tunneling electrons in field emission.¹⁹ The enhancement of electron emission was also observed from gated Si field-emitter arrays, with irradiation of 100 mW yttrium aluminum garnet (YAG) laser at a wavelength of 532 nm.²⁰ However, there are few reports on the study of laser assisted field emission from nanostructures.

Recently, Xu *et al.* reported that white light illumination was able to effectively enhance the field emission current of CuO nanobelts.²¹ In the experiment, light generated from a halogen lamp was used to irradiate the sample through a transparent anode and an increase in emission current (up to 19%) was recorded. The observation was attributed to extra carriers induced by photons. Similarly, ultraviolet (UV) illumination has been found to be able to enhance the field emission current of a single ZnO nanowire by two orders of magnitude.²² In these preliminary reports, however, the effects of a few factors such as wavelength of light, irradiation intensity, surface adsorption, etc., remain unclear. To better elucidate the interplay among these contributing factors, it is worthwhile to carry out systematic studies of the light-induced enhancement in field emission. In this work, we conduct detailed studies on laser irradiation enhanced field emission from CuO nanowire films with continuous wavelength (CW) lasers. The effects of factors such as laser wavelength, power density, time response, emission current, and working pressure are discussed and a model is proposed to account for the laser irradiation enhanced emission process.

II. EXPERIMENTAL METHOD

Aligned CuO nanowire films were synthesized by directly heating Cu plates on a hotplate at around 450 °C in

^{a)}Author to whom correspondence should be addressed. Electronic mail: physowch@nus.edu.sg

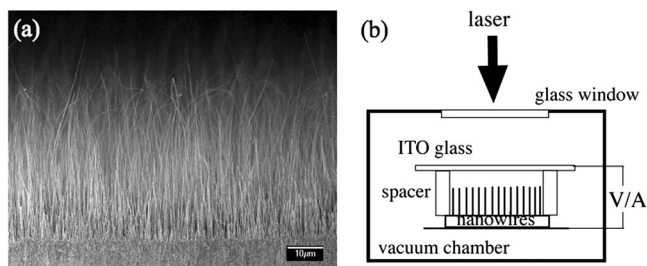


FIG. 1. (a) Typical cross-sectional SEM of as-grown CuO nanowire arrays. (b) Setup for the laser enhanced field emission study.

ambience, as described in our previous report.³ Temperature and heating duration could be varied to control the diameter and length of nanowires.⁸ After cooling down, as-grown CuO nanowires were peeled off from the substrate and Fig. 1(a) shows a typical scanning electron microscope (SEM, JEOL 6400F) image of CuO nanowires from a side view. The length of nanowires is around 40 μm and the average tip diameter is between 80 and 100 nm. The density of nanowires is about 10⁸/cm². As-grown CuO nanowires were attached to another clean Cu plate by copper tape as field emission cathode. An indium tin oxide (ITO) coated glass slide was used as anode and cover glass slides (100 μm thick) were used as spacers. Figure 1(b) schematically shows the field emission measurement setup in the vacuum chamber. To study the effect of vacuum, two different chambers, with base pressures of $\sim 6 \times 10^{-7}$ and $\sim 3 \times 10^{-9}$ Torr, respectively, were employed. During the field emission measurement, laser beams from CW lasers with different wavelengths and intensities were irradiated on the surface of nanowire films *in situ* through the transparent ITO glass anode. The spot size of laser beam varied from 4.8 to 95 mm² for different lasers. All irradiation intensity was normalized with the spot size, after consideration of the power lost through the viewing window of the chamber and the ITO anode. Current versus voltage or time response of current was recorded by a Keithley 237 high voltage source measurement unit. For time response studies, laser on/off was controlled by simply unblocking/blocking the laser beam with a shutter. Five different lasers were employed in this work. The wavelengths of the laser beam emitted by these lasers are 405, 532, 808, 1064, and 1550 nm. From here on, we shall denote the laser that emits laser beam with a wavelength of 405 nm as 405 nm laser and so on. Among the lasers used, the power of 532 and 1064 nm lasers is tunable and used to investigate the effect of irradiation intensity. To rule out the possible contribution from the ITO glass, a control field emission experiment was carried out with irradiation on the glass surface only and no enhancement was observed. Furthermore, in the study of each parameter, the same sample was used and other experimental conditions were kept exactly the same to avoid any influence of sample variation or measurement process. The optical adsorption band gap of CuO nanowires was measured with UV-visible spectrometer (Shimadzu UV-3600) by dispersing the nanowires in ethanol.

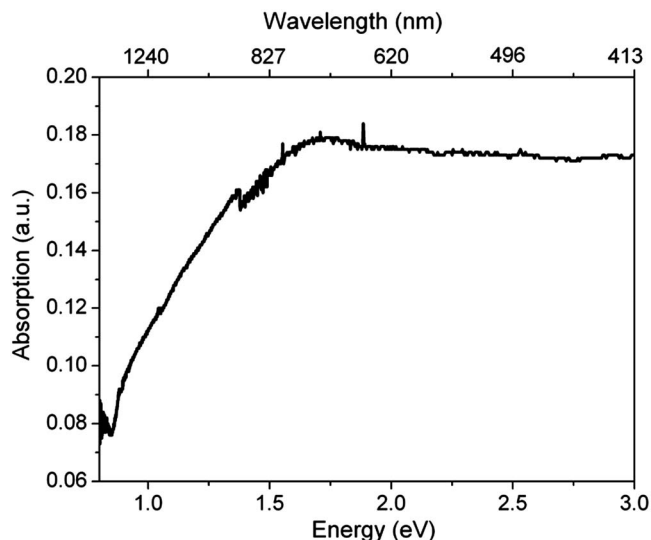


FIG. 2. Photoabsorption spectrum of CuO nanowires in absolute ethanol solvent.

III. EXPERIMENTAL RESULTS

The reported band gap of CuO has a wide distribution,^{9–12} which is sensitive to the morphology, structure, and chemical purity as well. Compared with their bulk counterpart, nanowires could also exhibit different optical properties due to the effects from their large specific surface area. Thus it is important to characterize our nanowire samples. Figure 2 shows the optical absorption spectrum of as-grown CuO nanowires in absolute ethanol after correcting for background contribution from the solution. A broad and linear absorption edge can be observed from the spectrum, ranging from 0.9 eV (~ 1378 nm) to 1.7 eV (~ 729 nm). For the photon energy larger than 1.7 eV the absorption remains nearly constant until 3 eV (413 nm). Such a result is obviously wider than the range of 1.2–1.7 eV, mainly from CuO films. The broad band gap distribution could be due to the wide distribution of nanowire diameter or different crystalline structures.²³

Figure 3 shows the result of enhanced field emission from CuO nanowire films by 532 nm laser irradiation. From the current density versus applied electric field (J - E) curves in Fig. 3(a), we can see that, with the irradiation of a very low laser power density of 75 mW/cm², the emission current has been improved significantly. When the intensity reaches the output limit of the 523 nm laser, around 792 mW/cm², the emission current continues to increase without any sign of saturation. The inset of Fig. 3(a) shows the time response of the current with the laser irradiation on or off under a fixed applied field (6.7 V/μm). If we define the dark current density as J_d and the current density with laser irradiation as J_i , an enhancement ratio α ($\alpha = (J_i - J_d)/J_d$) of 67% can be achieved with the irradiation intensity of 792 mW/cm². In addition, the response of the current increase upon irradiation was less than 1 s, faster than the switching of laser, which was manually controlled by a shutter. In Fig. 3(b), the time response of current density with different irradiation intensities was compared. Obviously, the absolute enhancement increased with the increase in the irradiation intensity. At the

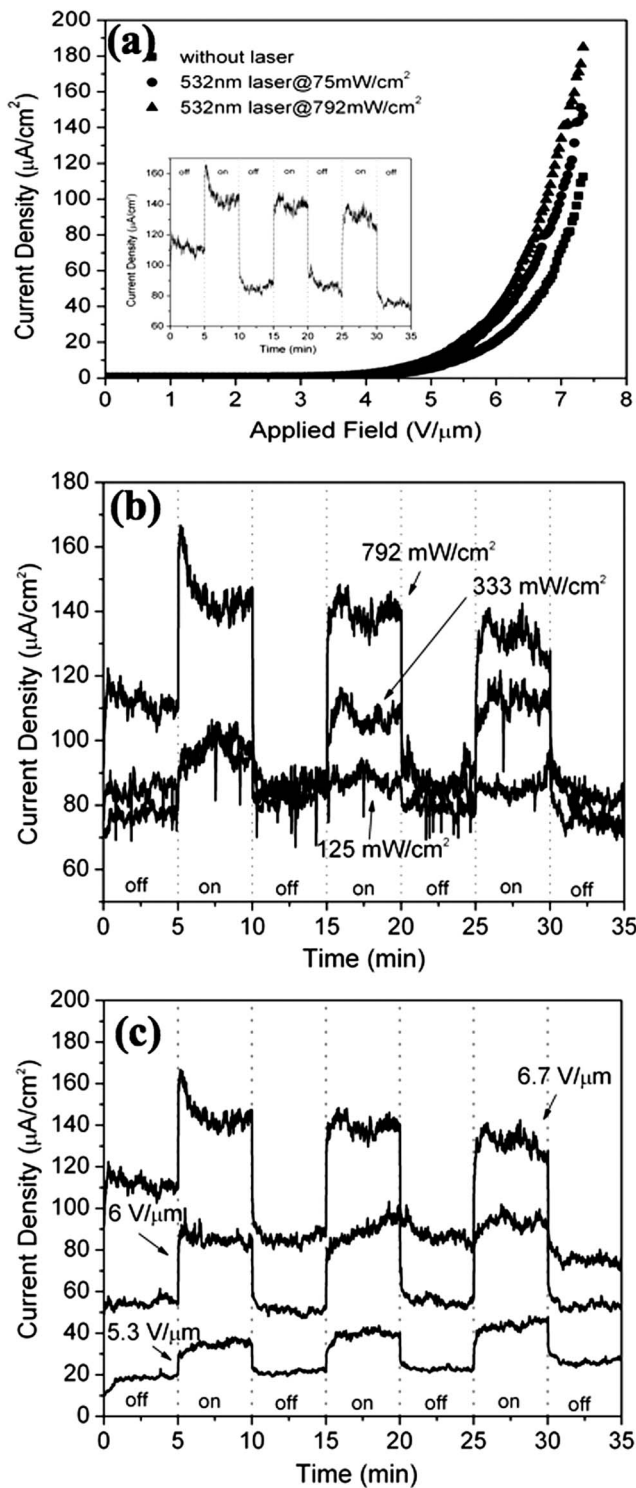


FIG. 3. (a) Typical field emission $J-E$ curves of CuO nanowire arrays with or without 532 nm laser irradiation. Inset shows the time response of current density under fixed electric field ($6.7 \text{ V}/\mu\text{m}$) subject to on and off the laser irradiation with power density of $792 \text{ mW}/\text{cm}^2$. (b) Time response of current under 532 nm laser irradiation with different power densities. (c) Time response of current under 532 nm laser irradiation under different electric fields.

same time, the estimated average enhancement ratios α are about 8%, 31%, and 67% for the intensities of 125, 333, and $792 \text{ mW}/\text{cm}^2$, respectively. Furthermore, α depends on the applied field and thus the initial dark current density, as shown in Fig. 3(c). With the increase in the initial current,

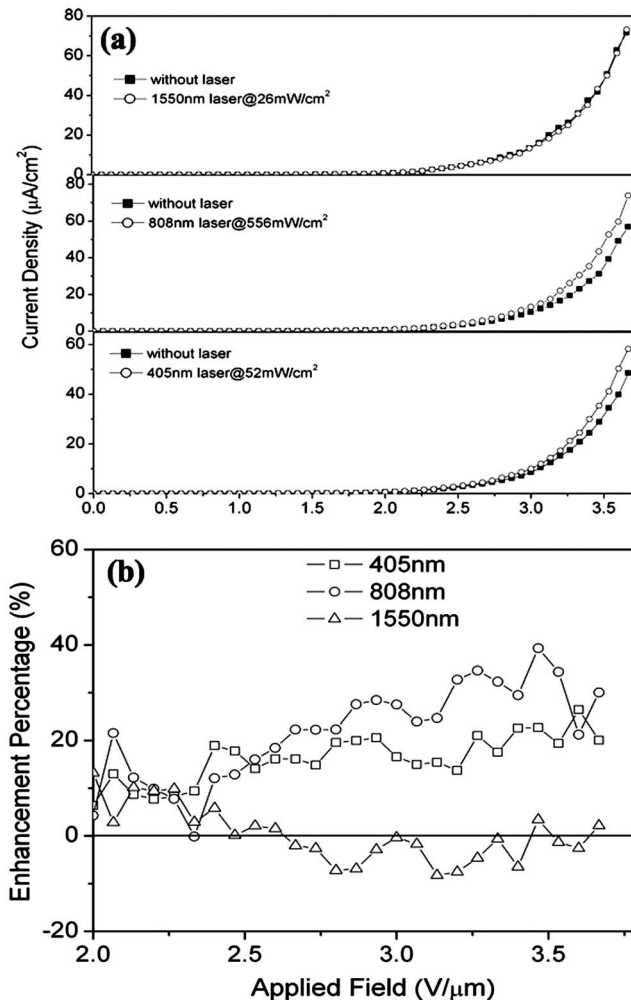


FIG. 4. (a) Field emission enhancement under the irradiation of laser with wavelengths of 1550, 808, and 405 nm. (b) Emission current enhancement vs applied field for different laser wavelengths.

the absolute enhancement increased correspondingly with the same irradiation intensity of $792 \text{ mW}/\text{cm}^2$. However, α value decreases from about 82% to 73% and finally 67% for the average dark currents of 22, 52, and $84 \mu\text{A}/\text{cm}^2$ respectively. Another trend we can see from Fig. 3(c) is that, for small initial current density, the dark current shows a gradual increase after the irradiation is switched off. On the contrary, for higher initial current, e.g., that under $6.7 \text{ V}/\mu\text{m}$, the dark current shows a decreasing trend. As for the intermediate one, the background current is more or less a constant. Furthermore, for the irradiation of $792 \text{ mW}/\text{cm}^2$ under the field of $6.7 \text{ V}/\mu\text{m}$, a rapid increase in current was observed in the first peak, followed by a significant decrease. Such a phenomenon was not observed in other cases with lower intensity of irradiation or small dark current.

The laser irradiation enhanced field emission was investigated with different laser wavelengths. Figure 4(a) shows the $J-E$ curves from another sample with or without irradiation of lasers with wavelengths of 405, 808, and 1550 nm. From the curves we can see that 1550 nm laser did not have any remarkable effect on the field emission of CuO nanowires, while both 405 and 808 nm lasers can enhance the emission current effectively. To demonstrate the difference

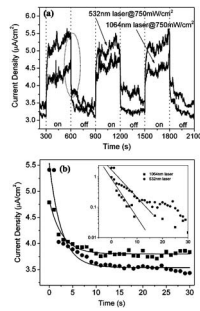


FIG. 5. (a) Comparison of effect of lasers with the same power density but different wavelengths. (b) Magnified decay edge marked in (a). Decay time factors of 2.7 and 2.6 s can be obtained by fitting the first 60 s data for 1064 and 532 nm laser irradiations. Inset of (b) shows the semilog plot after subtracting the background.

more clearly, based on the data from J - E curves, α values for each wavelength have been plotted as a function of applied field, as shown in Fig. 4(b). Considering the larger current fluctuation under low applied field, α values were shown only for the field higher than the turn-on field (around $2 \text{ V}/\mu\text{m}$). Again, 1550 nm laser gave no enhancement on the field emission and the enhancement ratio for 405 and 808 nm lasers can be higher than 20%.

The effect from different wavelengths was investigated with more details based on the time response of emission current with irradiations of 532 and 1064 nm lasers. Figure 5(a) shows the results obtained under the same intensity of around $750 \text{ mW}/\text{cm}^2$ and similar initial current density. Clearly, with the same intensity of irradiation, the enhancement induced by 532 nm laser is larger than that from 1064 nm laser. Furthermore, besides the rapid process immediately after the presence or absence of the laser irradiation, a slower increase or decrease process was also observed from the time response curves in Fig. 5(a). Figure 5(b) shows the decay details as marked region in Fig. 5(a) and exponential decay fitting was carried out on the two curves. The decay was also shown with the semilog plotting in the inset after subtracting the background. Two similar time constants for the slow process, namely, 2.7 and 2.6 s, were obtained from the fitting. Although the time constants are different for different measurement circles, most results gave a typical time scale of a few seconds.

The second time scale increase or decrease suggests that surface adsorption or desorption related processes may occur upon switching on or off the laser irradiation, in addition to the fast photoelectronic process. To investigate the effect of surface adsorption, experiments were conducted at different environmental pressures for the same wavelength of 532 nm. Figure 6 shows the results obtained from the same sample in the same chamber but at two different pressure ranges of 10^{-9} and 10^{-7} Torr, respectively. To trace the surface related process, continuous I - E scans were carried out at these two pressures. In both cases, one voltage sweep (scan) without laser irradiation was followed by a few runs of scans with sustained irradiation with fixed intensity. After that, the irradiation was blocked and more runs were conducted until the curve reverted back to the first one. From Fig. 6(a) we can see that in ultrahigh vacuum, upon the first irradiation, the

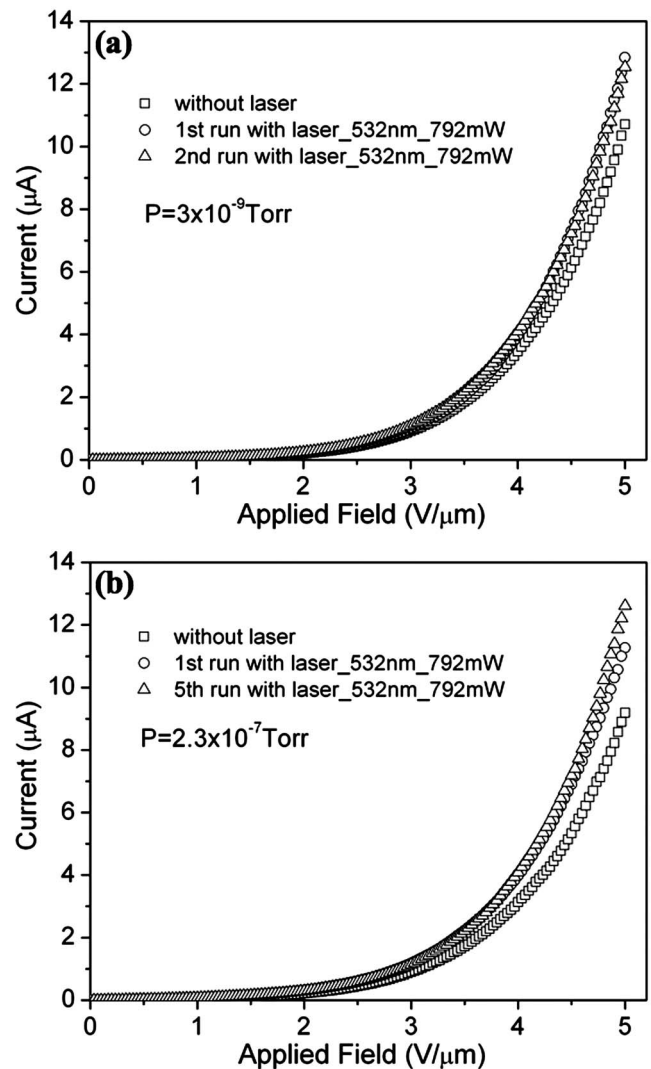


FIG. 6. (a) Continuous I - E curves under high vacuum. (b) I - E curves under lower vacuum.

enhancement has reached its maximum readily and subsequent runs just repeated the result of the first run with laser irradiation. On the contrary, in a poorer vacuum environment, Fig. 6(b) shows that first run with laser irradiation only enhanced the field emission to certain degree. The enhancement in field emission continued in subsequent runs until the fifth run, in which the enhancement reached a maximum. Similarly, upon blocking irradiation, a few runs were needed before the current recovered to the original values. Since a large number of field emission scans (or annealing) have been carried out to ensure that the emission current was stable before the pressure in the chamber was changed, such a difference is believed to be related to the oxygen adsorption/desorption on the surface of nanowires, as discussed later.

IV. DISCUSSION

From the experimental results shown above, we can see that the laser wavelength, irradiation intensity, dark current, and vacuum conditions have obvious influences on field emission performance of CuO nanowires. From these factors

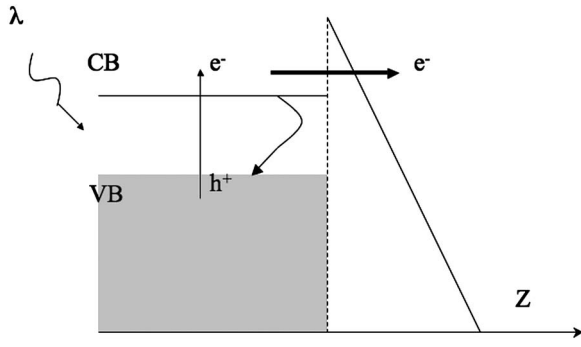


FIG. 7. Schematic showing laser irradiation assisted field emission process.

some physical mechanisms can be proposed and discussed. Basically, three main possible effects induced by laser irradiation are photon excitation, surface cleaning, and heating. Laser induced heating could result in temperature increase on the surface of nanowires, leading to more free electrons in the conduction band or even thermionic emission. However, considering the fact that the highest laser power density used in the experiments was less than 1 W/cm^2 , thermal effects can be ruled out from the mechanisms contributing to the emission current enhancement during laser irradiation. In a previous report,²⁰ it was proposed that thermal effect of illumination can be disregarded even for an irradiation intensity of 10^3 W/cm^2 . Thus extra electrons excited by incident photons and laser induced surface cleaning should be the main contributing factors responsible for the laser enhanced field emission from CuO nanowires. This may reasonably explain why 1550 nm laser irradiation did not enhance the field emission to any observable extent. In fact, the photon energy of 1550 nm ($\sim 0.8 \text{ eV}$) is below the band gap range (0.9–1.7 eV) of as-grown CuO nanowires, resulting in a very low absorption by the nanowires. In the following parts, we will discuss these two mechanisms.

A. Extra electrons excited by photons

During the laser irradiation, photons absorbed by nanowires can excite electron transitions from the valence band to the conduction band of CuO. A portion of the excess electrons may drift to the surface of nanowire and tunnel through the barrier between the nanowires and vacuum by field emission process. Figure 7 schematically shows the process of excess electron generation, followed by surface drifting and field emission. In a semiconductor, the field emission current can be expressed as²⁴

$$J = \frac{4\pi q m_t k_B T}{h^3} \int T(E_x) \ln[1 + e^{-(E_x - E_F)/k_B T}] dE_x$$

$$= J_0 \int T(E_x) N(E_x) dE_x = J_0 J_T. \quad (1)$$

Here $J_0 = 4\pi q m_t k_B T / h^3$, which represents the electron supply. $J_T = \int T(E_x) N(E_x) dE_x$ is defined as the tunneling factor of the field emission structure, q unit charge, m_t electron transverse mass, k_B is Boltzmann's constant, $E_x = P_x^2 / 2m$ normal energy, T is temperature, h is Planck's constant, and E_F is Fermi energy. Since the temperature is not remarkably changed by

laser irradiation, J_T decides the field emission current and enhancement. Among the factors determining J_T , both tunneling function T and supply function N are normal energy E_x dependent and thus affected by the incident photons. T can be calculated by the transfer matrix (TM) method, which is more dependent on the potential barrier.^{25,26} Thus we simplify J_T as $J_T = TN$ and only consider the excess electrons induced by photoexcitation.²⁰ Photoexcitation increases the number of electrons in conduction band as ΔN , which is determined by the balance between generation rate G by photons, emission increase $\Delta J = T\Delta N$, and recombination rate $r\Delta N(N + \Delta N)$ of electron-hole pairs so as to satisfy

$$G \approx T\Delta N + r\Delta N(N + \Delta N). \quad (2)$$

Thus, the enhancement ratio α is given by

$$\alpha = \frac{\Delta N}{N} \propto \frac{G}{NT + rN(N + \Delta N)},$$

$$\approx \frac{G}{J_T(1 + r\Delta N/T) + J_T^2(r/T^2)}. \quad (3)$$

Here r and $N + \Delta N$ are the recombination coefficient and number of holes in the valence band. In this case, J_T is also the dark current without laser irradiation. Furthermore, in the photoexcitation process we have²⁷

$$G \propto \frac{\sigma P}{h\nu}, \quad (4)$$

where σ is the adsorption coefficient, P the irradiation power density, and $h\nu$ the incident photon energy.

From Eqs. (3) and (4) we can see that the emission enhancement ratio α is proportional to the irradiation intensity for the same laser wavelength. The enhancement ratio from Fig. 3(b) was plotted in Fig. 8(a) as function of 532 nm laser power density. The data points can be fitted with a straight line passing through the origin, suggesting that the excess electrons excited by laser irradiation can be reasonably considered as one of main contributions for enhanced field emission current. On the other hand, Eq. (3) suggests that under the irradiation with the same intensity, the enhancement ratio decreases with the increase in the dark current. This point roughly agrees well with the experimental results in Fig. 3(c). More α values obtained from Fig. 3(a) (792 mW/cm^2) were also plotted as a function of dark current in Fig. 8(b). It can be seen that when the current is higher than $60 \mu\text{A/cm}^2$, the enhancement ratio shows a constant decrease with the increase in the current. For the low current, the fluctuation of current and other contributions such as tunneling function T make the estimate based on Eq. (3) inaccurate. Although no obvious saturation was observed in the measurements, Eq. (3) indicates that α will decrease rapidly when dark current is large enough. This case corresponds to the situation where the supply function N is large enough and the tunneling factor T is the main limiting factor in the field emission process. It is worth noticing that here the dark current N includes the contributions from both conduction band and valence band. Considering the large density of states in the valence band of CuO,²⁸ the tunneling of electrons from the valence band could be dominant. Such a mechanism may explain why the

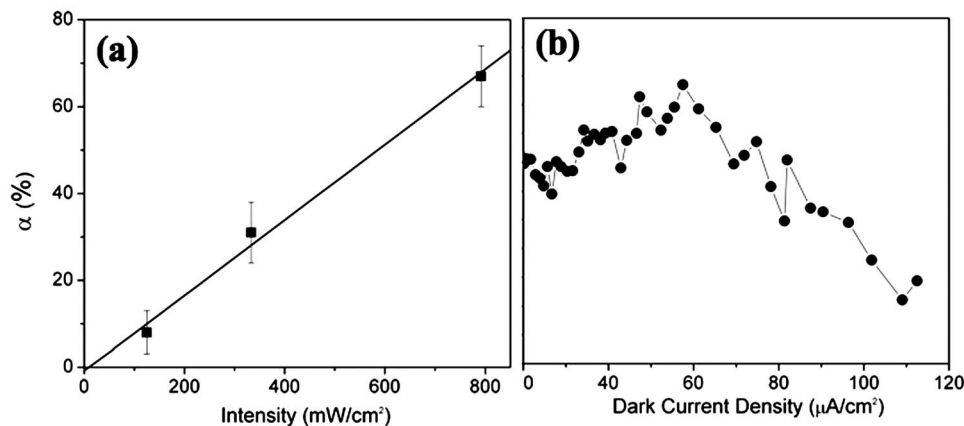


FIG. 8. Field emission enhancement ratios as function of (a) laser power density and (b) dark current density.

photoinduced current increase is undetectable when the emission current is higher than certain value, as reported by Chen *et al.*²¹ In addition, for the laser with higher photon energy, the extra energy could increase the density of electrons at higher energy levels in conduction band, increasing the tunneling probability of excited electrons and thus the emission current. This could be one of the contributing factors for the observation that 532 nm laser irradiation produced a higher enhancement ratio α than 1064 nm laser [Fig. 5(a)], besides their different absorption coefficients. Finally, in current work the effect of dark current and wavelength has to be discussed based on average effect since the actual local field and current were unknown for those nanowires involving field emission. More accurate relationship could be obtained by studying the effect of laser irradiation on the field emission from single nanowire.

B. Surface desorption

Apart from the rapid photoexcitation process discussed above, other surface related process could occur during the laser irradiation, as suggested by the slow decay in Fig. 5(b). Laser irradiation may induce some surface cleaning effects such as oxygen desorption from the CuO nanowires.²⁹ It has been widely accepted that the *p*-type characteristic of CuO is mainly due to excess oxygen ions or copper ion vacancies.³⁰ The oxygen adsorption/desorption related electric property of CuO nanowires has been reported for the application of gas sensors.³¹ Laser assisted oxygen desorption may decrease the carrier density and the conductivity of nanowires. Such a decrease in the carrier density is responsible for the sharp current decrease following the rapid increase upon laser irradiation, as shown in the first peak in the inset of Fig. 3(a). With continuous irradiation of high intensity ($792 \text{ mW}/\text{cm}^2$), the background current kept decreasing, as shown in Fig. 3(b). High emission current induced self-heating may also result in surface desorption,³² so the same effect could occur when a higher electric field was applied on the nanowires [Fig. 3(c)]. On the other hand, the readsorption of oxygen will dominate once laser irradiation is blocked, especially for the case under poorer vacuum conditions. The interplay of laser assisted oxygen desorption and readsorption has resulted in different behaviors for field emission measured in ultrahigh vacuum and poorer vacuum, as shown in Fig. 6. In Fig. 6(a), under ultrahigh vacuum the

first *I-E* scan has increased the emission current to the maximal and stable runs were observed thereafter. Here the laser desorption rate is much higher than oxygen readsorption rate. On the contrary, in poorer vacuum [Fig. 6(b)], only after the fifth run did the *I-E* curve reach steady state, suggesting no further significant oxygen desorption related carrier density decrease after the fifth run. Here the invariance of the voltage sweep corresponds to the equilibrium established between desorption and readsorption rates. Such an oxygen adsorption affected field emission was also observed from the individual ZnO nanowires.²² However, this is different from the case for CuO nanowires, as oxygen adsorption reduces the carrier density and thus field emission current of *n*-type ZnO nanowires.

V. CONCLUSION

Field emission from CuO nanowire films has been investigated *in situ* with laser irradiation. The effects of irradiation intensity, wavelength, dark current, and environmental pressure on the enhancement were studied. It was found that photoexcitation by incident laser beam is responsible for the enhancement and laser assisted surface desorption plays an important role as well. Based on the field emission theory of semiconductor, a process was proposed and discussed to explain the experimental observations. This phenomenon can be used to fabricate optical sensors or switches based on the field emission of CuO nanowires.

ACKNOWLEDGMENTS

The authors acknowledge the support from the National University of Singapore Academic Research Fund. Y.W.Z. thanks C.F. Cheong and K. S. Yeong for their help in experiments.

¹N. S. Xu and S. E. Huq, *Mater. Sci. Eng., R.* **48**, 47 (2005).

²C. T. Hsieh, J. M. Chen, H. H. Lin, and H. C. Shih, *Appl. Phys. Lett.* **83**, 3383 (2003).

³Y. W. Zhu, T. Yu, F. C. Cheong, X. J. Xu, C. T. Lim, V. B. C. Tan, J. T. L. Thong, and C. H. Sow, *Nanotechnology* **16**, 88 (2005).

⁴X. Jiang, T. Herricks, and Y. Xia, *Nano Lett.* **2**, 1333 (2002).

⁵T. Yu, X. Zhao, Z. X. Shen, Y. H. Wu, and W. H. Su, *J. Cryst. Growth* **268**, 590 (2004).

⁶W.-Y. Sung, W.-J. Kim, S.-M. Lee, H.-Y. Lee, Y.-H. Kim, K.-H. Park, and S. Lee, *Vacuum* **81**, 851 (2007).

⁷Y. W. Zhu, A. M. Moo, T. Yu, X. J. Xu, X. Y. Gao, Y. J. Liu, C. T. Lim, Z. X. Shen, C. K. Ong, A. T. S. Wee, J. T. L. Thong, and C. H. Sow,

- Chem. Phys. Lett. **419**, 458 (2006).
- ⁸C. H. Teo, Y. W. Zhu, and C. H. Sow, J. Nanosci. Nanotechnol. (to be published).
- ⁹J. Ghijsen, L. H. Tjeng, J. V. Elp, H. Eskes, J. Westerink, G. A. Sawatzky, and M. T. Czyzyk, Phys. Rev. B **38**, 11322 (1988).
- ¹⁰F. Marabelli, G. B. Parravicini, and F. Salghetti-Drioli, Phys. Rev. B **52**, 1433 (1995).
- ¹¹W. Y. Ching, Y.-N. Xu, and K. W. Wong, Phys. Rev. B **40**, 7684 (1989).
- ¹²F. P. Kottlyberg and F. A. Benko, J. Appl. Phys. **53**, 1173 (1982).
- ¹³J. Chen, S. Z. Deng, N. S. Xu, W. Zhang, X. Wen, and S. Yang, Appl. Phys. Lett. **83**, 746 (2003).
- ¹⁴P. Samarasekara, M. A. K. M. Arachchi, A. S. Abeydeera, C. A. N. Fernando, A. S. Disanayake, and R. M. G. Rajapakse, Bull. Mater. Sci. **28**, 483 (2005).
- ¹⁵J. S. Kim, K. S. Ahn, C. O. Kim, and J. P. Hong, Appl. Phys. Lett. **82**, 1607 (2003).
- ¹⁶S. M. Huang, Z. Sun, C. W. An, Y. F. Lu, and M. H. Hong, J. Appl. Phys. **90**, 2601 (2001).
- ¹⁷J. T. Lee and W. L. Schaich, Phys. Rev. B **38**, 3747 (1988).
- ¹⁸M. J. Hagmann, IEEE Trans. Microwave Theory Tech. **52**, 2361 (2004).
- ¹⁹M. J. Hagmann, J. Vac. Sci. Technol. B **13**, 1348 (1995).
- ²⁰H. Ishizuka, Y. Kawamura, K. Yokoo, H. Mimura, H. Shimawaki, and A. Hosono, Nucl. Instrum. Methods Phys. Res. A **483**, 305 (2002).
- ²¹J. Chen, N. Y. Huang, S. Z. Deng, J. C. Chen, N. S. Xu, W. Zhang, X. Wen, and S. Yang, Appl. Phys. Lett. **86**, 151107 (2005).
- ²²K. S. Yeong, K. H. Maung, and J. T. L. Thong, Nanotechnology **18**, 185608 (2007).
- ²³B. AGizhevskii, Y. P. Sukhorukov, N. N. Loshkareva, A. S. Moskin, E. V. Zenkov, and E. A. Kozlov, J. Phys.: Condens. Matter **17**, 499 (2005).
- ²⁴R. Tsu and L. Esaki, Appl. Phys. Lett. **22**, 562 (1973).
- ²⁵J. Q. You, L. D. Zhang, and P. K. Ghosh, Phys. Rev. B **52**, 17243 (1995).
- ²⁶R. Z. Wang, X. M. Ding, B. Wang, K. Xue, J. B. Xu, H. Yan, and X. Y. Hou, Phys. Rev. B **72**, 125310 (2005).
- ²⁷S. O. Kasap, *Principles of Electronic Materials and Devices*, 3rd ed. (McGraw-Hill, New York, 2006).
- ²⁸D. Wu, Q. Zhang, and M. Tao, Phys. Rev. B **73**, 235206 (2006).
- ²⁹R. J. Chen, N. R. Franklin, J. Kong, J. Cao, and T. W. Tomblor, Appl. Phys. Lett. **79**, 2258 (2001).
- ³⁰V. F. Drobny and D. L. Pulfrey, Thin Solid Films **61**, 89 (1979).
- ³¹C. Wang, X. Q. Fu, X. Y. Xue, Y. G. Wang, and T. H. Wang, Nanotechnology **18**, 145506 (2007).
- ³²H. Z. Zhang, R. M. Wang, and Y. W. Zhu, J. Appl. Phys. **96**, 624 (2004).